Cell. Mol. Life Sci. 66 (2009) 156 – 172
1420-682X/09/010156-17
DOI 10.1007/s00018-008-8490-7

Cellular and Molecular Life Sciences

Research Article

Differential insult-dependent recruitment of the intrinsic mitochondrial pathway during neuronal programmed cell death

S. Diwakarla[a,b], P. Nagley[c], M. L. R. Hughes[c,d], B. Chen[a] and P. M. Beart[a,b,*]

[a] Brian Injury and Repair Program, Florey Neuroscience Institutes, The University of Melbourne, Parkville, Victoria 3010 (Australia), Fax: +61 3 9347 0446, e-mail: philip.beart@florey.edu.au
[b] Department of Pharmacology, The University of Melbourne, Parkville, Victoria 3010 (Australia)
[c] Biochemistry and Molecular Biology, PO Box 13D, Monash University, Victoria 3800 (Australia)
[d] Victorian College of Pharmacy, Monash University, Parkville, Victoria 3052 (Australia)

Received 14 August 2008; received after revision 02 October 2008; accepted 23 October 2008
Online First 8 November 2008

Abstract. Programmed cell death contributes to neurological diseases and may involve mitochondrial dysfunction with redistribution of apoptogenic proteins. We examined neuronal death to elucidate whether the intrinsic mitochondrial pathway and the crosstalk between caspase-dependent/-independent injury was differentially recruited by stressors implicated in neurodegeneration. After exposure of cultured cerebellar granule cells to various insults, the progression of injury was correlated with mitochondrial involvement, including the redistribution of intermembrane space (IMS) proteins, and patterns of protease activation. Injury occurred across a continuum from Bax- and caspase-dependent (trophic-factor withdrawal) to Bax-independent, calpain-dependent (excitotoxicity) injury. Trophic-factor withdrawal produced classical recruitment of the intrinsic pathway with activation of caspase-3 and redistribution of cytochrome c, whereas excitotoxicity induced early redistribution of AIF and HtrA2/Omi, elevation of intracellular calcium and mitochondrial depolarization. Patterns of engagement of neuronal programmed cell death and the redistribution of mitochondrial IMS proteins were canonical, reflecting differential insult-dependencies.

Keywords. Cell death, neurons, excitotoxicity, mitochondrial membrane potential, Bax, proteases, cytochrome c, AIF.

Introduction

Mammalian cells possess a multiplicity of "death" pathways that can contribute to programmed cell death (PCD), including apoptosis, and the essential functions of many pro-apoptotic molecules render cells "at risk" to the diverse challenges that threaten cellular homeostasis. Apoptosis contributes to the neuropathology associated with various neurodegenerative disorders (e.g. Alzheimer's and Parkinson's disease, and amyotrophic lateral sclerosis) [1]. Further, mitochondrial dysfunction plays a key role in inducing apoptotic cell death in these conditions [2]. Apoptotic execution is generally accompanied by caspase activation, which occurs either directly via the "extrinsic" cell surface pathway or through the "intrinsic" mitochondrial pathway. The intrinsic pathway involves the redistribution of mitochondrial cytochrome c (cyt c) to the cytosol, apoptosome

* Corresponding author.

formation, and activation of caspase-9 triggering downstream events involving "executioner" caspases [3]. Additionally, several other cell death inducers are translocated from the mitochondrial intermembrane space (IMS) to the cytosol, namely second mitochondrial activator of caspases/direct IAP binding protein with low pI (Smac/DIABLO) and high temperature requirement protein A2/Omi stress regulated endoprotease (HtrA2/Omi). Both proteins promote caspase-9 activation by neutralizing the caspase inhibitory properties of the inhibitor of apoptosis protein (IAP) family. In contrast, apoptosis-inducing factor (AIF), an NADH oxidoreductase, translocates to the nucleus and triggers caspase-independent cell death, and its role in neuronal injury is poorly understood. AIF has dual functions which may involve cellular resistance to oxidative stress through maintenance of complex I (compromised in Parkinson's disease; [4]) and mediation of chromatin condensation and DNA fragmentation [5, 6].

An essential feature of IMS protein release is the permeabilization of the outer mitochondrial membrane (OMM), although mechanisms of protein export remain unclear. One theory involves opening of the mitochondrial permeability transition pore (mPTP), resulting in swelling of the mitochondrial matrix and rupture of the OMM (reviewed by [7]). These changes coincide with a reduction of mitochondrial membrane potential ($\Delta\Psi_m$), a phenomenon observed in some models of apoptosis and excitotoxic neuronal death [8, 9]. However, OMM rupture has been predominantly observed in isolated mitochondria, but its occurrence in mitochondria within intact cells has rarely been demonstrated [10]. Currently, mitochondrial IMS proteins are believed to escape via membrane pores or channels formed by the pro-apoptotic proteins Bax or Bak alone, or perhaps involving lipid components of the OMM [6, 11] in a $\Delta\Psi_m$-independent manner [6, 10]. Nevertheless, mPTP-mediated swelling of the IMM may facilitate release of IMS proteins through the permeabilized OMM (reviewed in ref. [10]).

Neurons clearly manifest these canonical death processes, but the range of stresses to which this specialized cell type is exposed does not always invoke "classical" apoptotic death. Thus, sequestration of mitochondrial Ca^{2+} has been linked to excitotoxic neuronal injury and models of ischemic brain injury, which are believed to involve caspase-independent cell death [12–15]. In addition, Ca^{2+} can induce mPTP opening [16] and activate enzymes, such as calpains, which share specificity for caspase substrates and interact with apoptogenic proteins to induce a caspase-independent mechanism of injury [5, 17]. In particular, there is evidence that calpain activation precedes the mobilization of AIF [17]. Early evidence for differential, system-dependent crosstalk between the caspase cascade and alternative cell death pathways [14, 18, 19] needs to be considered in the context of recent advances in our understanding of PCD, particularly its relevance to neuronal injury (see reviews [12, 15, 20]). This shift in awareness to a holistic concept of interplay between multiple injury mechanisms explains the existence of cellular events quite different to classical PCD (PCD Type 1 = apoptosis [21]). Such an array of diverse "death" responses occurs across the apoptotic-necrotic continuum with different biochemical and morphological signatures reported both *in vitro* and *in vivo* (dubbed "pathological apoptosis"), and is consistent with plasticity of cell death activation dependent upon cell type and injury paradigm [12, 15, 20].

How this spectrum of cell death involving interactive crosstalk applies to neuronal PCD remains to be fully elucidated. Our specific aims were to determine whether injury mechanisms common to neurologic conditions (oxidative stress, excitotoxicity and neurotrophic deprivation [15]) induced PCD with the recruitment of the intrinsic mitochondrial pathway and the redistribution of IMS proteins. We used primary cultures of murine cerebellar granule cells (CGCs), an established *in vitro* model [22], exposed to various insults mimicking the above injury processes (collectively termed "neurologic stressors") to analyze the differential induction of PCD. Thus we compared the actions of the excitotoxin kainic acid (KA) and the oxidative stressor, hydrogen peroxide (H_2O_2), to those of staurosporine (STS), a widely used inducer of apoptotic neuronal cell death. Additionally, this model conveniently allows the parallel comparison of these different insults with trophic factor-dependent apoptosis [23]. Herein, we report insult-dependent engagement of death machinery with differential, canonical redistribution of IMS proteins, including AIF, providing new evidence for neuronal PCD involving a continuum of cell death responses.

Materials and Methods

Materials. Dialysed fetal calf serum and MEM were obtained from Gibco BRL Life Technologies (Melbourne, Australia). Poly-D-lysine, BSA, aphidicolin, KA, H_2O_2, KCl, MTT, Triton-X 100, paraformaldehyde, PI, DTT, FCCP, furosemide, dimethyl sulfoxide and z-VAD-fmk were purchased from Sigma-Aldrich (Sydney, Australia**).** STS was purchased from Tocris Cookson (Bristol, U.K.). Mouse monoclonal anti-β-actin IgG and HRP-conjugated affinity purified secondary antibodies were from Chemicon (Mel-

bourne, Australia). Fluo-3AM, Pluronic F-127, the secondary antibodies conjugated to Alexa 488, Alexa 568 and Alexa 647, mouse monoclonal anti-COX II IgG, CMXRos and TMRM were purchased from Molecular Probes (Eugene, OR, USA). Complete protease inhibitor cocktail and lumi light Western blotting substrate were from Roche Diagnostics (IN, USA). Mouse monoclonal anti-cyt c IgG (clone 6H2.B4 and 7H8.2C12) and mouse monoclonal anti-Bax IgG (clone 6A7) were purchased from BD Pharmingen (San Diego, CA, USA). Rat monoclonal anti-Smac/DIABLO IgG (clone 10G7) and rabbit polyclonal anti-HtrA2/Omi IgG were from Alexis Biochemicals (CA, USA). Goat polyclonal anti-AIF IgG was purchased from Santa Cruz Biotechnology (CA, USA). The rabbit polyclonal anti-Hsp60 antibody was a kind gift from Dr. Michael Ryan, La Trobe University. ALLM, calpastatin peptide, DEVD-fmk and LEHD-fmk were from Calbiochem (Sydney, Australia). Mouse monoclonal anti-α-fodrin was from Biomol (PA, USA).

Murine cerebellar granule cell cultures. All experimentation received ethical approval and was undertaken according to the guidelines of the NH&MRC (Australia). The establishment and characterization of primary cultures of CGCs from mouse cerebellum of seven day old Swiss White mice has been described previously [22]. CGCs were grown in Neurobasal medium containing B27 components, 25 mM KCl, 500 μM L-glutamine, and 100 U/ml penicillin-streptomycin (Gibco BRL Life Technologies, Melbourne, Australia). Cells were exposed to 10% dialysed fetal calf serum for the first 24 h and maintained in serum-free conditions from day *in vitro* (*div*) 1. CGCs were grown in NUNC™ plates (Denmark), pre-coated with poly-D-lysine (50 μg/ml), and maintained in a humidified CO_2/N_2 incubator (5% CO_2, 8.5% O_2, 37 °C). Aphidicolin (1 μg/ml) was added to the medium 18–24 h after plating to inhibit growth of non-neuronal cells [22]. These cultures have been previously shown to consist of > 95% neurons after immunocytochemical staining [22]. All experiments were performed at 7 *div.*

Induction of PCD and assessment of cell viability. Cultures (96 well plates, 0.12×10^6 cells/well) were exposed to varying concentrations of STS (1–1000 nM), KA (1–1000 μM), H_2O_2 (1–1000 μM), and KCl (0–25 mM) for 24 h. Different injury times (1–24 h) were examined with STS (100 nM), KA (100 μM), H_2O_2 (20 μM), and low K^+ (5 mM) in MEM containing 25 mM KCl (excepting low KCl treated cells) and these concentrations were used for all subsequent studies. Cell viability was determined at 24 h by the reduction of MTT, a measure of mitochondrial metabolic function [24]. MTT was added to cells at a final concentration of 0.5 mg/ml and incubated for 30 min at 37 °C. The reduced formazan product was lysed from the cells with dimethyl sulphoxide, and the absorbance was measured at 570 nm. Cells treated with 0.1% Triton-X-100 for 24 h were treated as 100% cell death and the results were expressed as percentage of the vehicle control (0% cell death). In some experiments, treatment of neurons with STS, KA, H_2O_2 and low K^+ was also performed in the presence of a broad spectrum caspase inhibitor (zVAD-fmk, 50 μM), a caspase-9 inhibitor (LEHD-fmk, 50 μM), a caspase-3 inhibitor (DEVD-fmk, 50 μM) and a calpain inhibitor (calpastatin peptide, 5 μM).

Assessment of PCD. Phosphatidylserine externalization, an early marker of apoptotic-like injury, was monitored by treating neurons (48 well plates, 0.2×10^6 cells/well) with insults for 15 min prior to a 15 min incubation at room temperature (RT) with Annexin V-FITC (2.5%; Molecular Probes, Eugene, OR, USA). To discriminate between early and late apoptotic cells, the membrane impermeable DNA binding dye, PI (10 μg/ml), was also added to cultures [24]. Representative images of Annexin V-FITC and PI labeled cells (488/510 nm and 535/617 nm, respectively) were captured using the Olympus U-TB190 fluorescence microscope over a period of 24 h. Positive staining of cells was expressed as a percentage of the total number of cells counted per image. Neurons pretreated for 1 h with zVAD-fmk (50 μM) prior to insult exposure were also assessed by PI labeling.

Intracellular calcium measurements. Change in intracellular calcium ($[Ca^{2+}]_i$) levels were determined using the fluo-3AM calcium-binding dye as previously described [24]. Neurons in 48 well plates were washed and loaded with 10 μM Fluo-3/AM, incubated for 1 h (37 °C) and washed with 1 mM furosemide to prevent efflux of the dye. Relative fluorescence of basal Ca^{2+} levels was immediately determined over 5 min using the Fluoroskan Ascent fluorometer (485/535 nm). Following measurements of basal levels cells were exposed to STS, KA, H_2O_2 and low K^+. Fluorescence was immediately measured over a 5 min time interval and results were standardized against basal values. Background fluorescence levels present in cells treated with buffer alone were subtracted from all samples at each time point and the change in $[Ca^{2+}]_i$ was represented as a percentage of the control.

Assessment of caspase-3 and -8 enzyme activity. Caspase-3 and -8 enzyme activity were measured fluorometrically using a caspase Activity Assay kit (Calbiochem, Australia), which measures the cleavage of DEVD and IETD substrates labeled with the fluorogenic molecule 7-amino-4-trifluoromethyl coumarin. Neurons in 96 well plates were processed according to the manufacturer's specifications. Caspase-3 and -8 activity were measured in relative fluorescence units (RFU; 390/510 nm) immediately after addition of the substrate conjugate (zero time point) and following a 2 h incubation period. Inclusion of assay buffer only controls and treated cells containing caspase-3 and -8 inhibitors ensured specificity of the assay. All results were standardized against buffer control wells to eliminate endogenous fluorescence and data were represented as a percentage of untreated controls.

Subcellular fractionation and Western immunoblotting. Cultures (6 well plates, 1.5×10^6 cells/well) were treated with insults for 0–24 h and cytosolic and mitochondrial fractions were obtained using a digitonin-based subcellular fractionation technique. Full details of fractionation and Western immunoblotting have been given elsewhere [24]. The antibody for HtrA2/Omi was found unsuitable for this technique.

Confocal imaging for mitochondrial protein redistribution. CGCs were seeded on glass coverslips precoated with poly-D-lysine (50 μg/ml) in 24 well plates (0.3×10^6 cells/well). Following exposure to insults cells were double immunostained as previously described [25]. Briefly, cells were fixed with 3.5% paraformaldehyde, permeabilized, and incubated for 1 h at 22 °C with 1% BSA (blocking solution). To simultaneously detect Smac/DIABLO and cyt c in cells, cultures were initially left for 1–2 days at 4 °C in blocking solution containing rat monoclonal anti-Smac/DIABLO antibody (1:100). Cells were incubated with a secondary antibody conjugated to Alexa 488 (1:200) overnight at 4 °C. After removal of the secondary antibody, cells were blocked with blocking solution and incubated with mouse monoclonal anti-cyt c antibody (clone 6H2.B4; 1:100) for 1–2 days. Cells were subsequently incubated with a secondary antibody conjugated to Alexa 568 (1:200) overnight at 4 °C. Concurrently, cells from the same culture were double immunolabeled with rabbit polyclonal anti-HtrA2/Omi (1:100) and goat polyclonal anti-AIF (1:100), followed by incubation with the secondary antibodies conjugated with Alexa 568 and 488, respectively. Immunostaining controls employed systematic removal of each primary and secondary antibody incubation step to ensure no cross-reactivity of antibodies [25]. Similar experiments were also conducted after cells were pretreated for 1 h with zVAD-fmk. Images were captured with the Leica TCS-NT inverted confocal microscope using a 100 × oil immersion objective lens (Leica, Adelaide, Australia). Double immunolabeling was also used to monitor Bax mobilization, where cells were fixed and permeabilized with 0.3% TX-100, and double immunolabeled with mouse monoclonal anti-Bax (1:100) and rabbit anti-Hsp60 (1:500) [24]. Under these conditions, all cellular Bax is detected, as TX-100 allows exposure of the antigen recognized by the monoclonal 6A7, irrespective of conformational changes on Bax activation.

Confocal analysis of mitochondrial polarization. Mitochondrial polarization was monitored using TMRM and CMXRos as described previously [24]. Briefly, CGCs grown on glass coverslips were loaded with CMXRos (50 nM) in phenol red-free MEM for 15 min. Cells were washed twice with MEM and exposed to insults over 24 h. Cultures were also treated with FCCP (10 μM), which acted as a positive control since it fully decreases fluorescence intensity [24] through its action as a mitochondrial uncoupler. Following apoptotic induction, cells were immediately washed with phosphate buffered saline (PBS) and fixed with 3.5% paraformaldehyde. Cells were mounted onto glass microscope slides and images were captured with the Leica TCS-NT inverted confocal microscope using a 100 × oil immersion objective lens. Untreated control samples for each time point were initially imaged and the same settings were used to acquire images for cells treated with STS, KA, H_2O_2, low K^+ and FCCP at the corresponding time points. With TMRM (150 nM), neurons were loaded for 15 min and washed as described above prior to the addition of insults containing 50 nM TMRM. A positive control sample (10 μM FCCP) was also employed. Live cell images were captured with a Zeiss L5M 5 PASCAL inverted confocal microscope using a 40× oil immersion lens (Carl Zeiss Pty Ltd, Sydney Australia).

Visualization of caspase-3 and calpain substrate cleavage products of α-fodrin. Cultures grown in 6 well plates were exposed to STS (100 and 200 nM) and KA (100 μM) for 0–24 h. Following induction of PCD, cells were washed and incubated for 15 min with 1 ml/well of RIPA buffer (50 mM Tris-HCl pH 7.4, 1% NP-40, 0.25% Na-deoxycholate, 150 mM NaCl, 1 mM EDTA, 1 mM PMSF, 1 mM Na_3VO_4, 1 mM NaF, 1 × protease inhibitor tablet). Cells were rocked on ice for 30 min and centrifuged at 14 000 × g for 15 min at 4 °C. Standard immunoblotting procedure was performed

using 8% sodium dodecyl sulfate-polyacrylamide gels. Membranes were probed with mouse monoclonal anti-α-fodrin (1:500) overnight at 4 °C and visualization of bands was performed using the ECL-Chemiluminescence system [24].

Data analysis. Data are given as a mean ± SEM. MTT assays were performed across five independent experiments measured in quadruplicate wells. For the detection of PS externalization and membrane integrity, experiments were performed across three independent cultures measured in duplicate wells. Representative images (four per well) were acquired for each insult over 24 h and no less than 1000 cells in total were scored per well for each time point. For the detection of mitochondrial protein redistribution by confocal microscopy, representative images (30 per well) were acquired for all insults studied over 0–24 h and individual data sets (n=4) were accumulated per time point for each protein from 250–500 cells in total. Quantitative measurements were also obtained from confocal images of neurons loaded with TMRM and CMXRos. Representative images (10 per well) were acquired for all insults studied over 24 h. The mean fluorescence intensity was measured across populations of neurons in control and treated groups using AnalySIS (Soft Imaging System; Olympus Soft Imaging, Melbourne, Australia) or Image J (http://rsb.info.nih.gov.ij). The mean (background) values obtained for the FCCP-treated group were first subtracted from those obtained for each of the vehicle-treated controls, and groups treated with insults. The adjusted values were then expressed as a percentage of corrected vehicle-treated control, which was designated to have 100% fluorescence. Graphs were generated using a computer-assisted curve fitting program (GraphPad Prism™) and statistical significance ($P<0.05$) of all data was examined by one- and two-way ANOVA, followed by Dunnett's *post hoc* test for intra-group comparison and Bonferroni's *post hoc* test to compare individual treatments.

Results

Diverse insults induce PCD, but KA-mediated injury triggers a rapid and early rise in intracellular calcium. Drug concentrations for inducing neuronal injury were determined by exposing CGCs to varying concentrations of STS, KA, H_2O_2 and low K^+ for 24 h (note that low K^+ simulates trophic factor withdrawal [23]). Insult exposure resulted in a concentration-dependent reduction to mitochondrial activity based on a decreased ability to metabolize MTT (data not shown). EC_{50} values: STS 36 ± 1 nM, KA 74 ± 1 μM, H_2O_2 22 ± 1 μM, and low K^+ 13 ± 2 mM. Concentrations inducing approximately 50% cell death were used for subsequent experiments. CGCs exposed to STS (100 nM), KA (100 μM), H_2O_2 (20 μM) and low K^+ (5 mM) all displayed time-dependent reductions in mitochondrial function (Fig. 1A). Light microscopic analyses of insult- but not vehicle-treated cultures revealed characteristics of apoptotic-like injury (neuritic blebbing, pyknosis and cell body shrinkage) with the complete absence of early necrotic-like swelling (data not shown; cf. refs [22, 26]).

Activation of injury pathways is often associated with an increase in cytosolic Ca^{2+} concentration [16]. Although STS and H_2O_2 produced negligible changes to intracellular Ca^{2+} levels ($[Ca^{2+}]_i$) relative to the vehicle-treated cultures, KA treatment caused a rapid and maintained rise in $[Ca^{2+}]_i$ (Fig. 1B), typical of excitotoxicity [27], which continued up to 2 h (data not shown). When CGCs were transferred to low K^+-containing medium, $[Ca^{2+}]_i$ levels were immediately reduced by 40% relative to control. No subsequent changes in $[Ca^{2+}]_i$ were observed with all stressors, including STS, when monitored over 24 h (data not shown).

Phosphatidylserine (PS) externalization represents an early upstream marker of apoptotic-like injury [24] and its labeling with Annexin V-FITC was evaluated after exposure to the various insults. Annexin V-FITC-positive cells were evident 1 h following STS, KA and low K^+ treatment and numbers increased in a time-dependent manner ($P<0.05$) relative to zero time controls (Fig. 1C). Significant labeling with H_2O_2 resulted at 2 h and by 4 h the pattern for KA was notably different to other stressors. We have previously reported DNA fragmentation under these conditions with KA [22]. Despite insult-dependent differences in labeling patterns, these data suggest ordered progression through cell injury.

Negligible PI labeling, following 1–2 h exposures to insults, was consistent with the early absence of necrosis [28]. Numbers of PI-positive cells found were low upon exposure to STS, H_2O_2 and low K^+ and were consistent with later alterations to membrane integrity. KA produced earlier incorporation of PI (32 ± 2%) at 4 h, indicating that some cells exhibited compromised membrane integrity (Fig. 1D). However, given the pattern of Annexin labeling and the maintained integrity of neuritic networks noted during KA exposure, PI labeling likely reflects secondary necrosis [29] or less likely aponecrosis [20]. These variations in timing of PI labeling suggested mechanistic differences in cell death that were dependent on the insult, although progression was always slow and ordered.

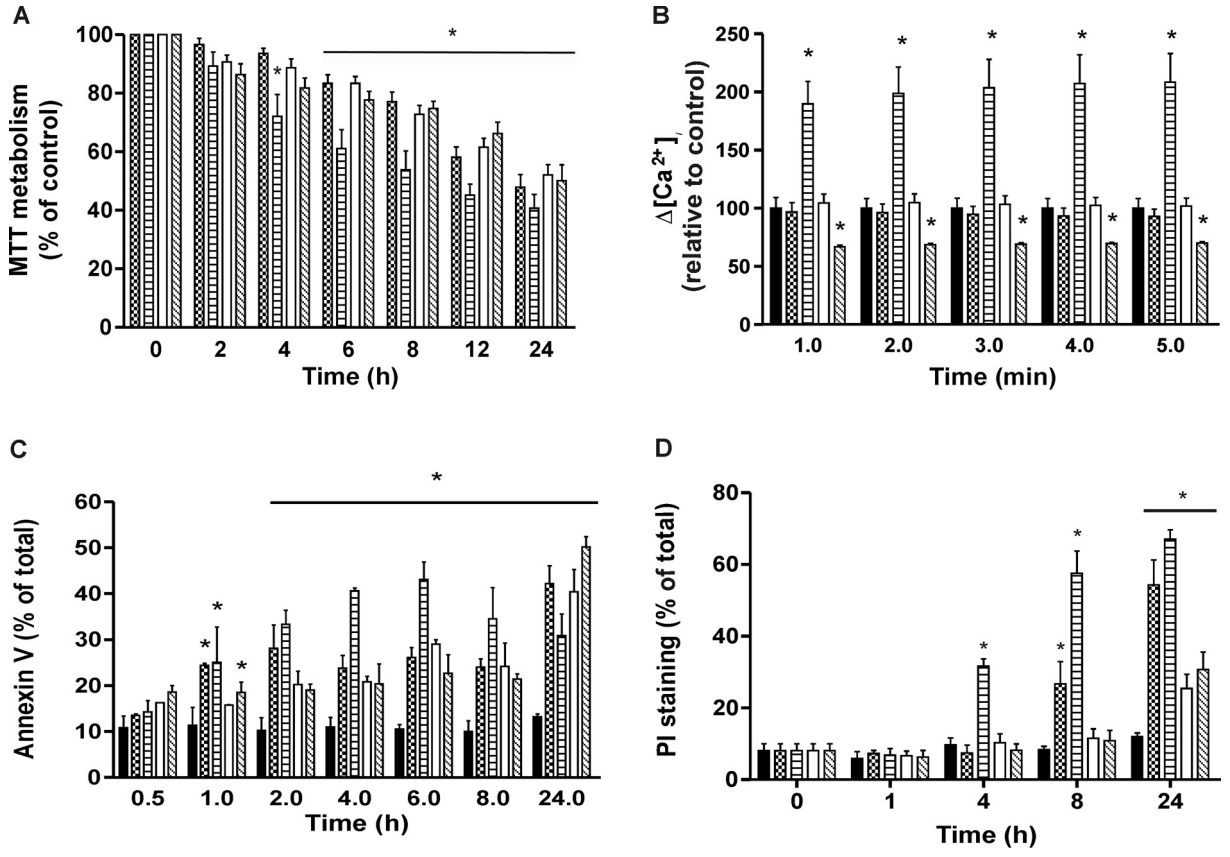

Figure 1. KA induces an early rise in $[Ca^{2+}]_i$ levels followed by a more rapid progression through to PCD when compared to other insults. (*A*) Cell viability was measured in CGCs treated with STS (100 nM; checked bars), KA (100 μM; horizontal bars), H_2O_2 (20 μM; white bars) and low K^+ (5 mM; diagonal bars) over 24 h using the MTT assay. Cell injury was found to be time-dependent. Values are the mean ± SEM of 5 independent experiments measured in quadruplicate and are expressed as a percentage of the control. (*B*) Intracellular Ca^{2+} levels were measured in CGCs treated with STS (checked bars), KA (horizontal bars), H_2O_2 (white bars) and low K^+ (diagonal bars) over 5 min using a quantitative fluorescence based assay. Data represent the mean ± SEM of five independent experiments measured in quadruplicate and are expressed as the percentage change in $[Ca^{2+}]_i$ relative to control. (*C*) Proportion of Annexin V-FITC-positive cells following STS (checked bars), KA (horizontal bars), H_2O_2 (white bars) and low K^+ (diagonal bars) was monitored over 24 h by fluorescence microscopy, and the proportion of cells staining positive were expressed as a percentage of the total number of cells counted per image (n = 300–500 cells). (*D*) Proportion of PI-positive cells during STS (checked bars), KA (horizontal bars), H_2O_2 (white bars) and low K^+ (diagonal bars) exposure over 24 h. Cells were labeled with PI following insult exposure and the proportion of cells staining positive for PI were expressed as a percentage of the total number of cells counted per image (n = 300–500 cells). Data represent the mean ± SEM of three independent experiments. Asterisks indicate statistical significance between control (black bars) and treated groups ($P<0.05$).

KA induces mitochondrial depolarization without early Bax translocation. Use of CMXRos represents a convenient method to monitor mitochondrial depolarization (loss of $\Delta\Psi_m$) since it is not irreversibly retained in neuronal mitochondria [24]. Moreover, use of CMXRos yielded essentially identical data to those obtained with the potentiometric dye TMRM. In untreated control cultures of CGCs in this work, CMXRos fluorescence was maintained over 24 h, and was rapidly reduced following treatment with FCCP (data not shown). CMXRos fluorescence in neurons treated with STS and H_2O_2 maintained similar levels to control cultures (data not shown), even though neurons displayed molecular and morphological alterations consistent with PCD. In contrast, KA-mediated injury induced an early and time-dependent decrease in CMXRos fluorescence, which was maintained over 8 h, while neurons treated with low K^+ displayed an increase in fluorescence intensity (data not shown). Given that alterations in $\Delta\Psi_m$ were only observed following KA and low K^+ treatment using CMXRos, live cell imaging of neurons loaded with TMRM [24] were conducted to provide further insights into $\Delta\Psi_m$ during these two injuries. Data with TMRM confirmed CMXRos results with KA inducing early and time-dependent reductions in fluorescence, while an overall increase in TMRM fluorescence intensity was observed after low K^+ exposure when compared to control cultures (Fig. 2A).

Insult-induced mobilization of Bax was confirmed by its co-localization with the mitochondrial matrix

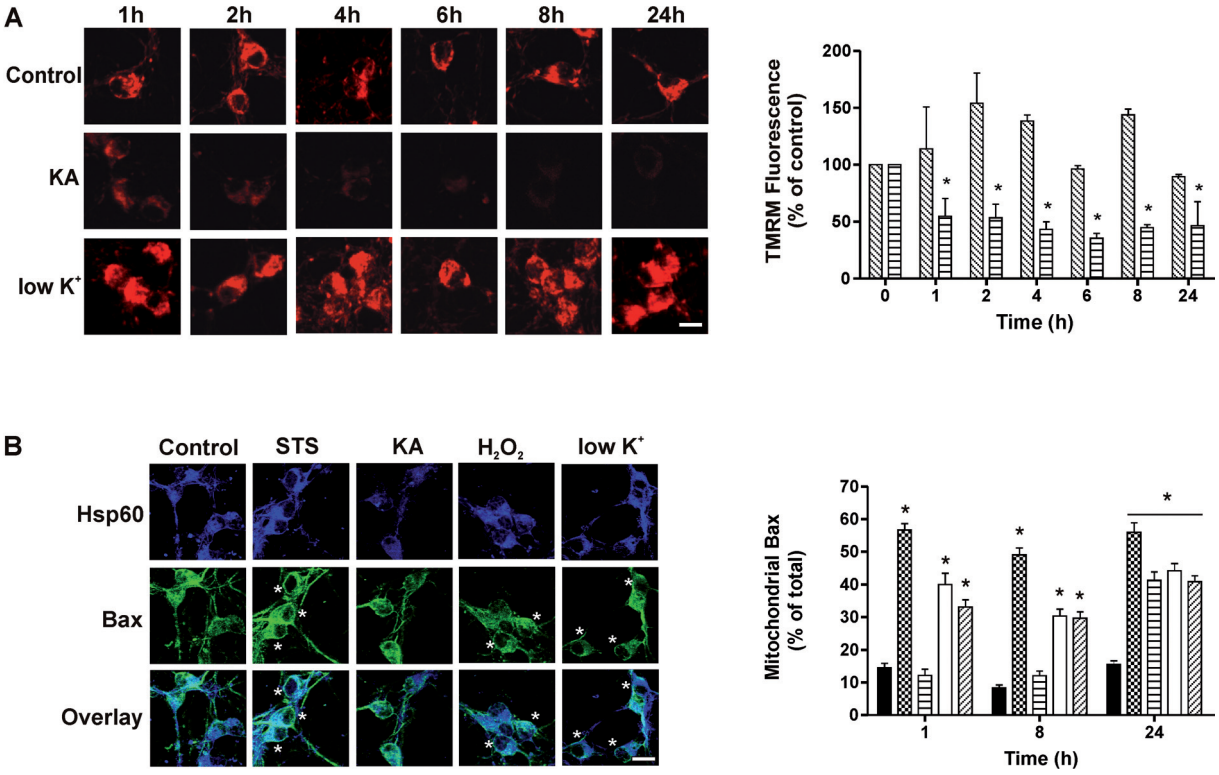

Figure 2. KA and low K^+ treatments alter mitochondrial membrane potential whereas STS and H_2O_2 are without effect. (*A*) Following exposure to KA (100 μM; horizontal bars) and low K^+ (5 mM; diagonal bars), cells were loaded with TMRM. Live cell confocal images of neurons loaded with TMRM were captured in untreated control cultures and cells treated with KA and low K^+. Scale bar = 10 μm. TMRM fluorescence is expressed as percentage of control (designated as 100 % fluorescence). All values have been corrected for residual TMRM fluorescence after FCCP treatment. Data represent the mean ± SEM of three independent experiments. Asterisks indicate significant loss of TMRM fluorescence at the indicated time points relative to control ($P < 0.05$). (*B*) STS, H_2O_2 and low K^+, but not KA, induced early recruitment of Bax to the OMM. Confocal images of control neurons and those treated with STS (100 nM; checked bars), KA (100 μM; horizontal bars), H_2O_2 (20 μM; white bars) and low K^+ (5 mM; diagonal bars) for 1 h after double immunostaining for hsp60 (a mitochondrial marker) and Bax. Asterisks indicate cells displaying mitochondrial localization of Bax, determined by co-localization of hsp60 (indigo) and Bax (green) immunofluorescence (generating a distinctive light blue colour, as opposed to the indigo colour of hsp60 alone). Note that under the conditions of immunostaining, all cellular Bax is bound by the antibody, not just activated Bax; see Materials and Methods herein and ref. [24]. Scale bar = 10 μm. Quantitative measurements of the proportion of cells scored positive for Bax and hsp60 redistribution. Data represent the mean ± SEM of 3 independent experiments (n = 500 cells per time point). Insult-dependent effects were observed ($P < 0.05$); asterisks indicate statistical significance between treated and control groups ($P < 0.05$).

protein hsp60 in double immunolabeled neurons [24]. In control CGCs, Bax immunofluorescence was homogenously distributed throughout cell bodies and nuclei, whereas hsp60 was localized exclusively in mitochondria (Fig. 2B). Thus, little or no co-localization of Bax and hsp60 immunofluorescence was detected in control CGCs. Quantitative analysis showed significant redistribution of Bax localization after a 1 h exposure to STS, H_2O_2, and low K^+, with approximately 60 %, 35 %, and 40 % of cells, respectively, exhibiting a punctate pattern of staining compared to untreated controls. In contrast, KA induced negligible Bax translocation at both 1 and 8 h when mitochondria were likely to be depolarized, although at 24 h 35–45 % of neurons stained positive for mitochondrial Bax recruitment (Fig. 2B). Overall, these results indicate that redistribution of Bax to the OMM is an early event in STS-, H_2O_2- and low K^+-mediated injury, and that the extent of recruitment is insult-dependent.

Immunocytochemistry reveals differential redistribution of IMS mitochondrial proteins. Two complementary strategies were employed as described previously to examine the redistribution of IMS proteins [24]. Western immunoblotting of cytosolic and mitochondrial fractions from CGCs served to confirm the identities of the IMS proteins redistributed by treatments. However, as in our previous work [24], Western blotting was not found to be a satisfactory approach for analysis of the precise timing of redistribution of individual proteins. Moreover, redistribution was not evidently accompanied by gross depletion of these proteins from the mitochondrial fraction (data not shown). Therefore, analyses of the kinetics and temporal pattern of protein redistribution were

undertaken using double immunolabeling and confocal microscopy [25]. In control cultures immunoreactivity for all proteins was distributed in the cytoplasm in a punctate pattern excluding the nucleus coincident with mitochondrial distribution in many cells (Fig. 3A). After exposure to the various insults, protein distribution became completely diffuse and cells were grouped according to their staining patterns [25].

Exposure of cells to insults induced time-dependent increases in mitochondrial protein redistribution with significant cyt c and Smac/DIABLO redistribution occurring as early as 2 h when compared to control CGCs. All treatments resulted in the relatively contemporaneous redistribution of both cyt c and Smac/DIABLO, consistent with both proteins sharing similar redistribution kinetics. STS treatment induced significant cyt c and Smac/DIABLO redistribution at 2 h (38 and 43%, respectively), with a maximum response at 6 h (51% and 55%, respectively). In contrast, HtrA2/Omi and AIF redistribution were more delayed, only reaching levels equivalent to that for cyt c and Smac/DIABLO at 6 and 12 h, respectively (Fig. 3B).

In contrast, KA-induced injury triggered a very different profile of protein redistribution. AIF was redistributed as early as 2 h, with approximately 60% of cells redistributing the protein compared to the control (Fig. 3B). The redistribution of HtrA2/Omi was also significantly higher than that of either cyt c or Smac/DIABLO, with approximately 30–35% more cells redistributing HtrA2/Omi and AIF, and these levels were maintained over 24 h. Overall, the timecourses of HtrA2/Omi and AIF redistribution were the same, indicating similar kinetics of redistribution (Fig. 3B). The early redistribution of HtrA2/Omi and AIF compared to cyt c and Smac/DIABLO indicates differential mechanistic patterns of protein redistribution.

In neurons treated with H_2O_2 significant redistribution of cyt c and Smac/DIABLO was observed at 2 h compared to control, whereas HtrA2/Omi and AIF were more delayed, but more advanced than found for STS and low K^+. Maximal redistribution of HtrA2/Omi and AIF was observed at 8 h, with approximately 60–65% of cells staining diffusely for these proteins. At 6–8 h of H_2O_2 redistribution of HtrA2/Omi and AIF predominated over the redistribution of cyt c ($P < 0.05$) and Smac/DIABLO (Fig. 3B).

Neurons exposed to low K^+ responded with significant redistribution of cyt c and Smac/DIABLO at 2 h, and maximal redistribution at 24 h. In contrast, the redistribution profiles for HtrA2/Omi and AIF were delayed ($P < 0.05$, 8 h) relative to cyt c and Smac/DIABLO (both $P < 0.05$). In particular, AIF redistribution was delayed throughout the 24 h timecourse when compared with cyt c, and only reached comparable levels to Smac/DIABLO at 12 h (Fig. 3B).

Redistribution of cyt c following H_2O_2 and low K^+ exposure was delayed compared to STS or KA ($P<0.05$), but essentially identical at later time points (12–24 h) except when compared to KA. The insult-dependent nature of protein redistribution was particularly evident during HtrA2/Omi and AIF redistribution. KA exposure resulted in early redistribution of both HtrA2/Omi and AIF relative to other insults between 2–4 h for HtrA2/Omi and 2–6 h for AIF, a pattern observed to a lesser extent with H_2O_2. Low K^+-exposure resulted in the delayed redistribution of HtrA2/Omi and AIF over 2–8 h, compared to other insults ($P<0.05$), and AIF redistribution was further delayed across 8–24 h when compared to STS and KA ($P<0.05$). Overall, these observations are consistent with evidence for the differential "tethering" and redistribution of IMS proteins in a stressor-dependent manner [10].

Caspase activation and inhibition. Caspase-3 activity, measured using the DEVDase procedure, was readily detected in neurons treated with most insults. Exposure of cells to STS and low K^+ produced time-dependent increases in caspase-3 activity ($P<0.05$). Significant elevations were observed at 4 h and levels continued to increase over 24 h when compared to control. In contrast, H_2O_2 induced minimal caspase-3 activation overall, although a significant elevation was observed at 24 h. Little evidence for prominent activation of caspase-3 was found for cells exposed to the excitotoxin KA (Fig. 4A). By comparison STS and low K^+ activated caspase-8 to a minor extent. Cells exposed to KA and H_2O_2 exhibited negligible caspase-8 activation (data not shown).

Caspase involvement was further investigated by monitoring downstream events using PI. Neurons pretreated with the broad spectrum caspase inhibitor zVAD-fmk were compared to cultures treated with insults alone (without zVAD-fmk). zVAD-fmk pretreatment reduced the number of PI-positive cells following STS, H_2O_2 and low K^+ exposure when compared to cultures treated without zVAD-fmk (Fig. 4B). STS-induced cell death was attenuated at 8 and 24 h, while zVAD-fmk delayed H_2O_2- and low K^+-mediated injury at 24 h. Consistent with preceding data zVAD-fmk provided minimal protection against cell death induced by KA.

The role of caspases following injury exposure was further explored by monitoring effects on the redistribution of IMS proteins [24]. CGCs were pretreated with zVAD-fmk, a caspase-9 inhibitor (LEHD-fmk) or a caspase-3 inhibitor (DEVD-fmk) prior to insult

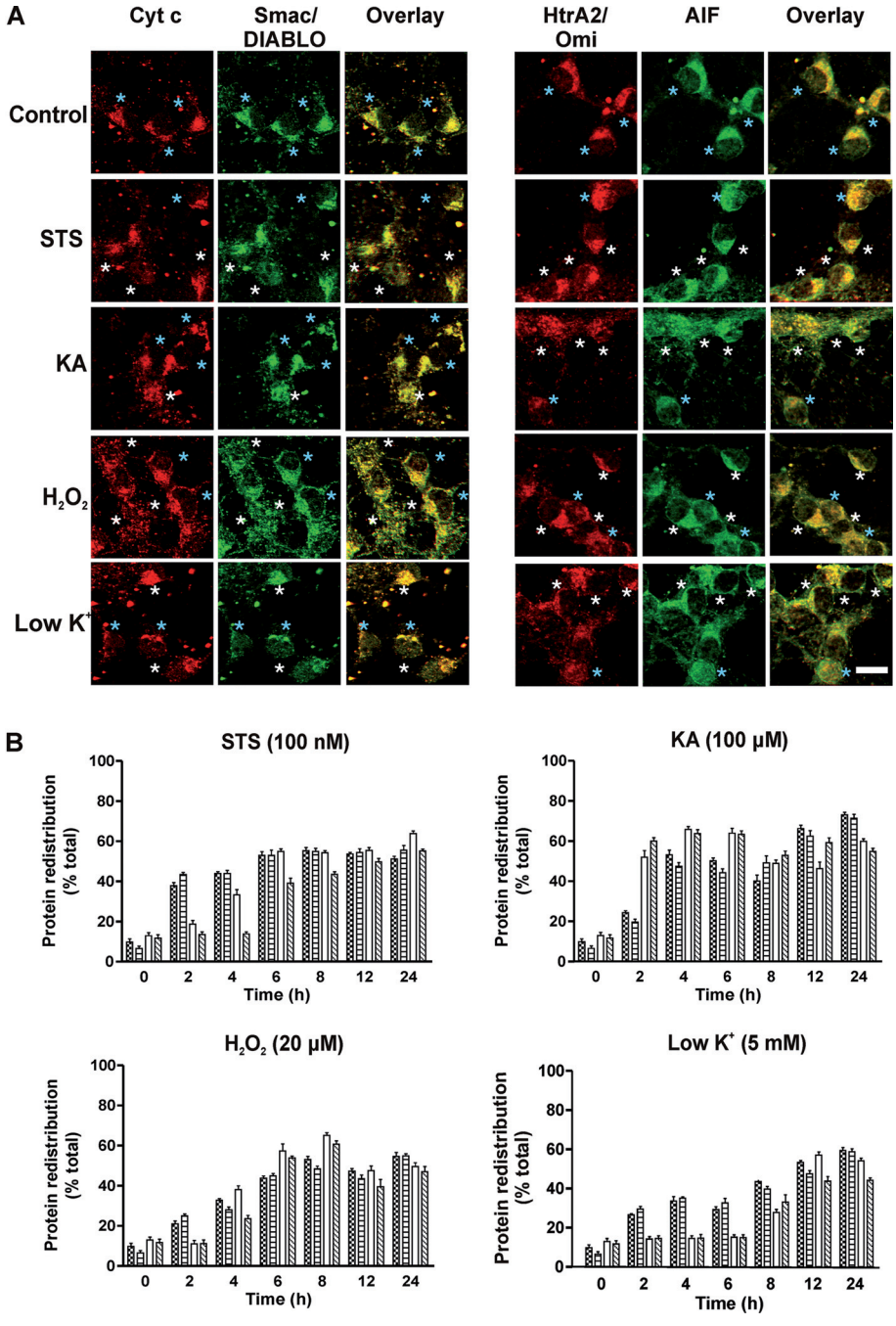

Figure 3. Mitochondrial redistribution of IMS proteins assessed by confocal microscopy after double immunocytochemistry. (*A*) Neurons were double immunolabeled with either cyt c and Smac/DIABLO or HtrA2/Omi and AIF following exposure to STS, H_2O_2, KA and low K^+ and fixation at various times. Untreated control cells displayed a punctate staining pattern, whereas treated cells that had redistributed protein from mitochondria displayed a diffuse staining pattern across the cell. Representative data are shown for CGCs exposed to various apoptotic stimuli at 2 h. Blue asterisks indicate mitochondrial localization of protein (no redistribution) and white asterisks indicate cytosolic distribution (redistribution). Scale bar = 10 µm. (*B*) STS, KA, H_2O_2 and low K^+ induce differential patterns of mitochondrial protein redistribution. Neurons were treated with STS, KA, H_2O_2 and low K^+. Data represent the overall proportion of cells scored for redistribution of cyt c (checked bars), Smac/DIABLO (horizontal bars), HtrA2/Omi (white bars), and AIF (diagonal bars) and are a mean ± SEM of four data sets. Data for each treatment group represent the mean proportion of cells scored for a particular redistribution profile out of the total number of cells counted (n = 250–500 cells). Each insult induced time-dependent protein redistribution ($P<0.05$).

exposure. zVAD-fmk exerted prominent actions on insult-induced redistribution of IMS proteins, especially Smac/DIABLO and to a lesser extent HtrA2/Omi (Fig. 4C). The effects of zVAD-fmk on STS treated cells resulted in minor, late effects on cyt c and Smac/DIABLO redistribution, and an appreciable reduction in HtrA2/Omi redistribution. These data suggest a possible caspase-dependent component of HtrA2/Omi redistribution. In contrast, AIF redistribution in zVAD-fmk pretreated cells was unchanged overall compared to insult alone controls, indicative of a caspase-independent mechanism herein. By comparison, with KA zVAD-fmk predominantly elevated the redistribution of Smac/DIABLO compared to cyt c, which was inhibited across midrange times. Overall, KA-induced redistribution of HtrA2/Omi increased when compared to cultures treated without zVAD-fmk, where as zVAD-fmk failed to affect the overall redistribution profile of AIF (Fig. 4C). Pretreatment of H_2O_2-treated cells with zVAD-fmk resulted in a small, but significant early increase in the number of cells redistributing cyt c when compared to insult only

controls. In contrast, at these times there was a greater increase in the number of cells releasing Smac/DIABLO. Overall, HtrA2/Omi and AIF redistribution were attenuated between 6–24 h ($P < 0.05$). However, in contrast to HtrA2/Omi, the number of cells redistributing AIF was biphasic displaying an early increase and late decrease (Fig. 4C). For low K^+ injury, caspase inhibition induced changes that generally paralleled those seen with STS with relatively minor effects on cyt c and, a greater increase in Smac/DIABLO redistribution and a late decrease in HtrA2/Omi (Fig. 4C). Negligible changes to cyt c redistribution were observed, confirming that under these experimental conditions release of cyt c is upstream of caspase activation. In contrast, Smac/DIABLO redistribution was observed to increase over all time points, with a maximum increase at 6 h. Further insights into protease involvement were sought by examining the redistribution of cyt c and AIF, proteins typically associated with caspase-dependent and caspase-independent PCD [4], respectively, following caspase-9 and caspase-3 inhibition. Specific caspase inhibition exerted little or no effect on the redistribution of IMS proteins (data not shown).

Calpain activation and inhibition. Neuronal injury caused by excitotoxicity induces calpain activation [17, 24, 30] and, given the apparent lack of caspase activation following KA-mediated excitotoxicity, we explored the activation of this Ca^{2+}-dependent protease. Immunoblot analyses were used to monitor the cleavage of α-fodrin, a substrate for calpain and caspase-3 during neuronal injury [31]. The cleavage of endogenous α-fodrin (240 kDa) to a 145/150 kDa breakdown product is indicative of calpain activity, whereas identification of a 120 kDa fragment reflects caspase-3 activation [31]. Minimal calpain breakdown products were detected for STS (100 nM) at early time points, whereas a higher concentration (200 nM) was needed to produce both calpain and caspase fragments maximally at 24 h (Fig. 5A). In contrast KA exposure failed to generate the caspase cleavage product, although the 145/150 kDa calpain fragment was visible at all time points.

Additionally, calpain involvement was examined using the calpain inhibitor, calpastatin peptide, previously shown to be neuroprotective in primary hippocampal and cortical neurons [30]. Calpastatin peptide failed to protect in STS treated CGCs (Fig. 5B), but markedly enhanced mitochondrial function following KA exposure ($P < 0.05$). KA produced a time-dependent decrease in cellular viability and calpastatin peptide attenuated the effects of KA neurotoxicity over 1–4 h (Fig. 5B). Interestingly, calpastatin peptide significantly delayed H_2O_2-mediated injury at later time points (29 % at 24 h; $P < 0.05$) and had negligible effects on low K^+-induced neurotoxicity (data not shown). These finding suggest a major role for calpains in KA-induced injury and its involvement in H_2O_2-mediated injury.

Given the preceding data, the actions of the calpain inhibitor calpastatin peptide were explored on the redistribution of the IMS proteins cyt c and AIF. Cyt c redistribution following KA- and H_2O_2-mediated injury was attenuated in the presence of calpastatin peptide at 8 h (Fig. 6). However, calpain inhibition also exerted an overall treatment effect ($P < 0.05$) on AIF redistribution induced by both KA and H_2O_2. Calpastatin peptide attenuated the early redistribution of AIF following KA exposure (60 % decrease at 2 h; Fig. 6), consistent with calpain-mediated AIF redistribution in excitotoxicity [17]. Calpastatin peptide also attenuated the redistribution of AIF following H_2O_2 exposure (40 % decrease at 8 h; Fig. 6). This effect was consistent with mitochondrial activity data indicating a neuroprotective effect following calpain inhibition, although once again the net effect was a delay of AIF redistribution. Interestingly, no effect on cyt c or AIF redistribution was observed following STS or low K^+ treatment in the presence of calpastatin peptide.

Discussion

PCD is now considered as an array of diverse responses [20] and thus the injury profile of neurons should reflect such a complexity of death paradigms downstream of the range of stresses that this unique cell type is subjected to in the pathologic milieu. Herein we analysed neuronal cell death resulting from stressors (trophic factor deprivation, oxidative stress and excitotoxicity) known to contribute to various neurodegenerative conditions [15] and examined how the recruitment of mitochondrial death signaling determined the signature of PCD. Regardless of the neurologic stressor employed, we found neuronal death exhibited slow-onset kinetics with differential progression through PCD (e.g. patterns of Annexin V and PI labeling) and with canonical redistribution of IMS proteins. Other new findings emergent from our investigations included evidence for the insult-dependent recruitment across a continuum of potentially destructive events of caspase-dependent and/or -independent signaling consistent with full or incomplete execution of the internal mitochondrial pathway. Our K^+-minimization trophic factor deprivation, like STS-induced PCD, was essentially Bax- and caspase-dependent with early redistribution of cyt c (i.e. classical recruitment of the "intrinsic" pathway).

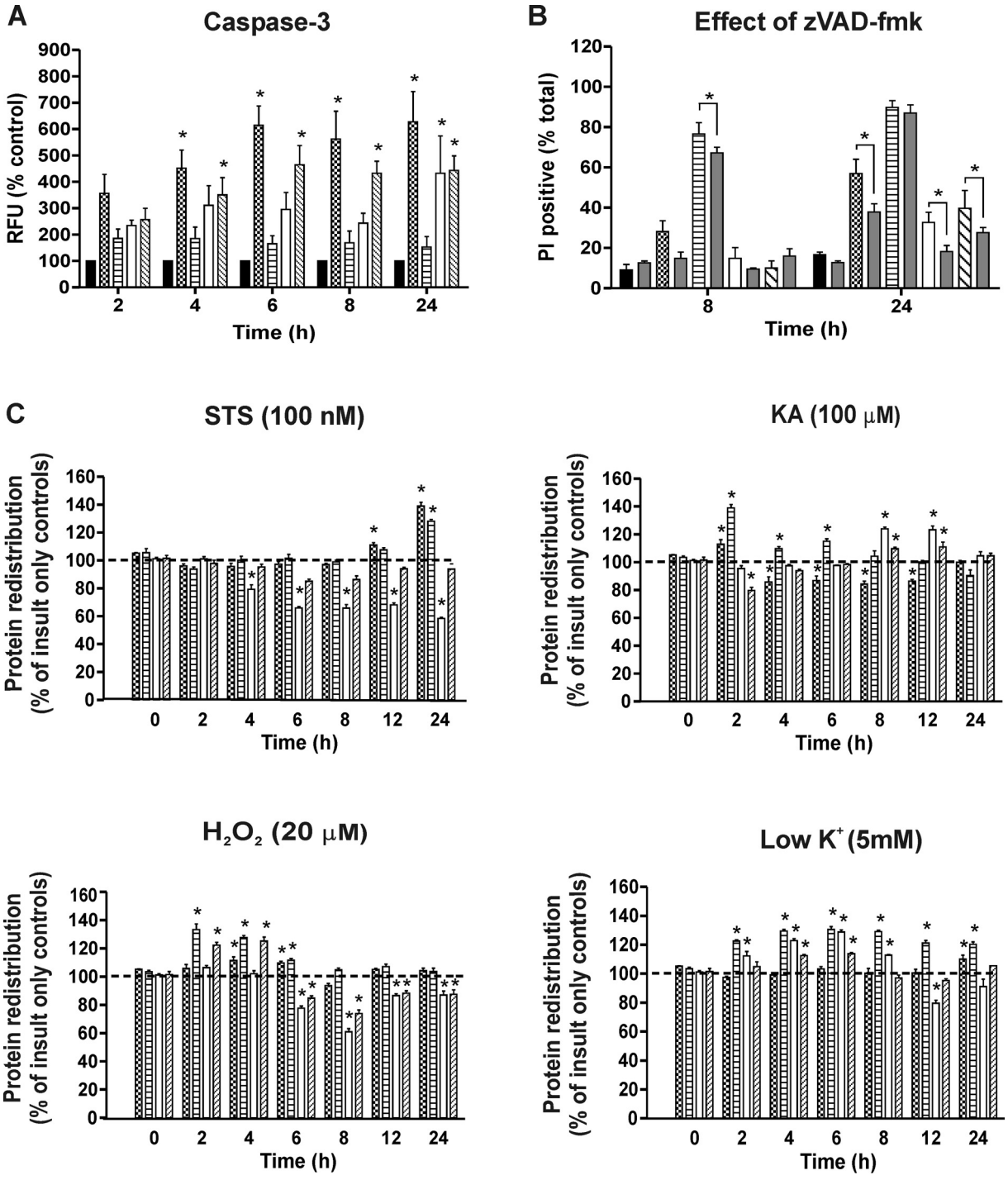

Figure 4. KA, unlike other insults, involves a caspase-independent mechanism of cell injury. (*A*) Elevation in caspase-3 activity following STS (checked bars), KA (horizontal bars), H_2O_2 (white bars) and low K^+ (diagonal bars) treatment over 24 h. Values are a mean ± SEM of three independent experiments measured in triplicate. (*B*) Neurons were treated with STS (checked bars), KA (horizontal bars), H_2O_2 (white bars) and low K^+ (diagonal bars) over 24 h in the absence and presence of zVAD-fmk (50 μM; grey bars) and labeled with PI. The proportion of cells staining positive for PI was expressed as a percentage of the total number of cells counted per image (n = 300–500 cells). Data represent the mean ± SEM of three independent experiments. Asterisks indicate significant differences relative to the appropriate control group ($P<0.05$). (*C*) Effect of zVAD-fmk on the timing of redistribution of IMS proteins. CGCs were treated with STS, KA, H_2O_2 and low K^+ and scored for protein redistribution of cyt c (checked bars), Smac/DIABLO (horizontal bars), HtrA2/Omi (white bars) and AIF (diagonal bars). The effect of zVAD-fmk on IMS redistribution is expressed as a percentage of insult only controls (dashed line). Data are mean ± SEM from four data sets, 250–500 cells/time point. Asterisks indicate significant differences from insult only controls ($P<0.05$).

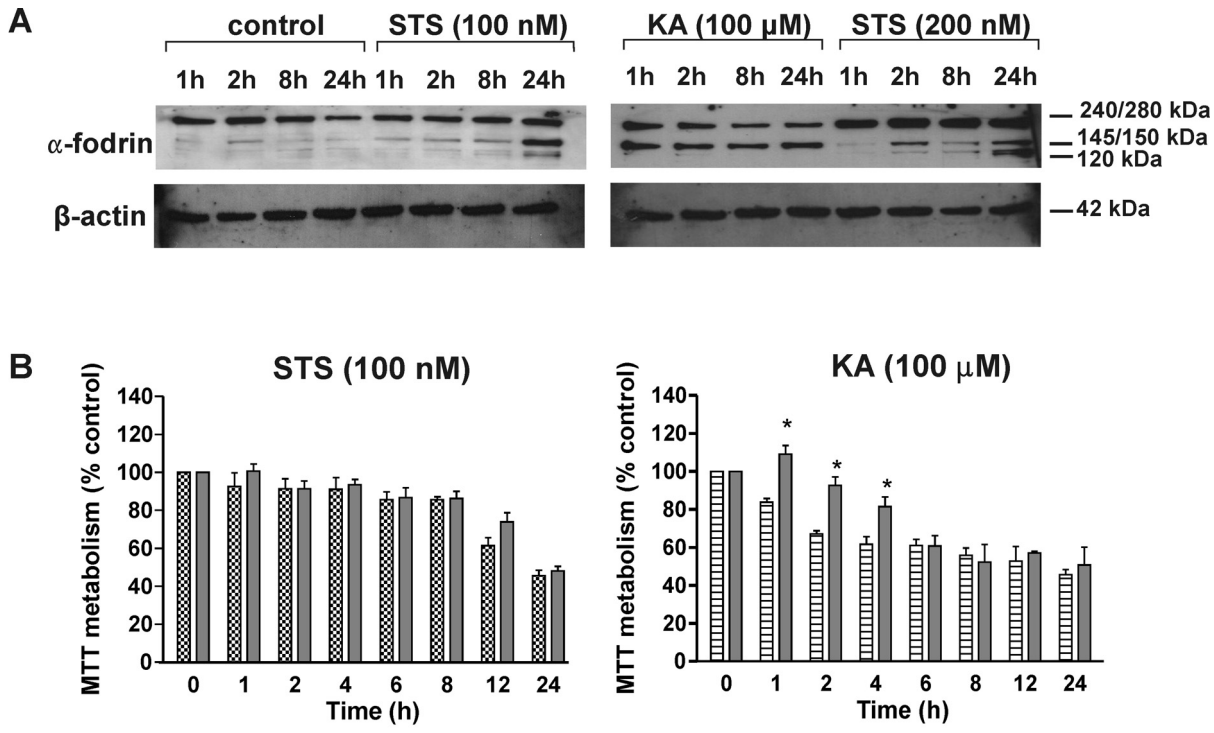

Figure 5. KA injury induces calpain activation and injury can be attenuated with calpain inhibitors. (*A*) Whole cell extracts of untreated neurons and cells treated with KA or STS were subjected to immunoblot analysis to visualize α-fodrin caspase and calpain breakdown products (1–24 h). STS induced both calpain and caspase cleavage products (145/150 kDa and 120 kDa, respectively), whereas KA-mediated injury induced early and prominent calpain cleavage fragments (145/150 kDa). Data are representative of three independent experiments. (*B*) Mitochondrial function determined by the MTT assay was monitored in the presence (grey bars) and absence of calpastatin peptide (5 μM) during treatment of neurons with STS (checked bars) or KA (horizontal bars) over a course of 24 h. Data represent the mean ± SEM of five independent experiments measured in quadruplicate and are expressed as percentage of control (100 % viability). Asterisks indicate significant differences relative to the appropriate control group ($P < 0.05$).

Oxidative stress typified by H_2O_2 exhibited an intermediate profile of Bax-dependent PCD involving both caspases and calpain indicative of interplay between cell death mechanisms. KA-mediated excitotoxicity was very skewed, the cell death being largely Bax-independent and calpain/AIF-dependent, but exhibited features of apoptosis, including membrane blebbing, DNA fragmentation and ordered redistribution of IMS proteins. Together these data indicate how the interactive dynamics between caspase-dependent/-independent PCD in neurons responds differentially to various influences (e.g. inhibition of one pathway, intensity of insult) in the adaptive milieu of death pathways (Fig. 7).

Evidence of mitochondrial involvement during STS-, KA-, H_2O_2- and low K^+-mediated injury. While there is strong evidence for mitochondrial participation during oxidative stress, trophic factor withdrawal and excitotoxicity based on the redistribution of IMS proteins, such as cyt c [32, 33], few studies have monitored the release of multiple proteins, especially in neuronal PCD. Here, an extensive analysis on the relative timing of IMS protein redistribution was undertaken, providing evidence on the kinetics and hierarchical nature of protein redistribution following OMM permeabilization. Mitochondrial protein redistribution was a general feature of PCD, where all insults induced redistribution of mitochondrial cyt c, Smac/DIABLO, HtrA2/Omi and AIF over a timeframe of 2–24 h. Moreover, differential recruitment of mitochondrial proteins and other cellular components involved in PCD was observed, indicating stimulus-dependent mechanisms of neuronal cell death (Fig. 7).

Low K^+ exposure, like STS resulted in apoptotic-like injury typical of caspase-dependent cell death, with the early redistribution of cyt c and Smac/DIABLO (2 h). These results indicate that under conditions of simulating trophic withdrawal or of kinase inhibition, cyt c is required for the apoptosome-mediated activation of caspase-3, while Smac/DIABLO may be released to promote cell death by inhibition of IAPs [34, 35]. The delayed redistribution of HtrA2/Omi and AIF suggested that these two proteins do not play a causative role in low K^+- and STS-induced PCD, but may further commit the cell to die and ensure completion of cell deletion. Although H_2O_2 triggered

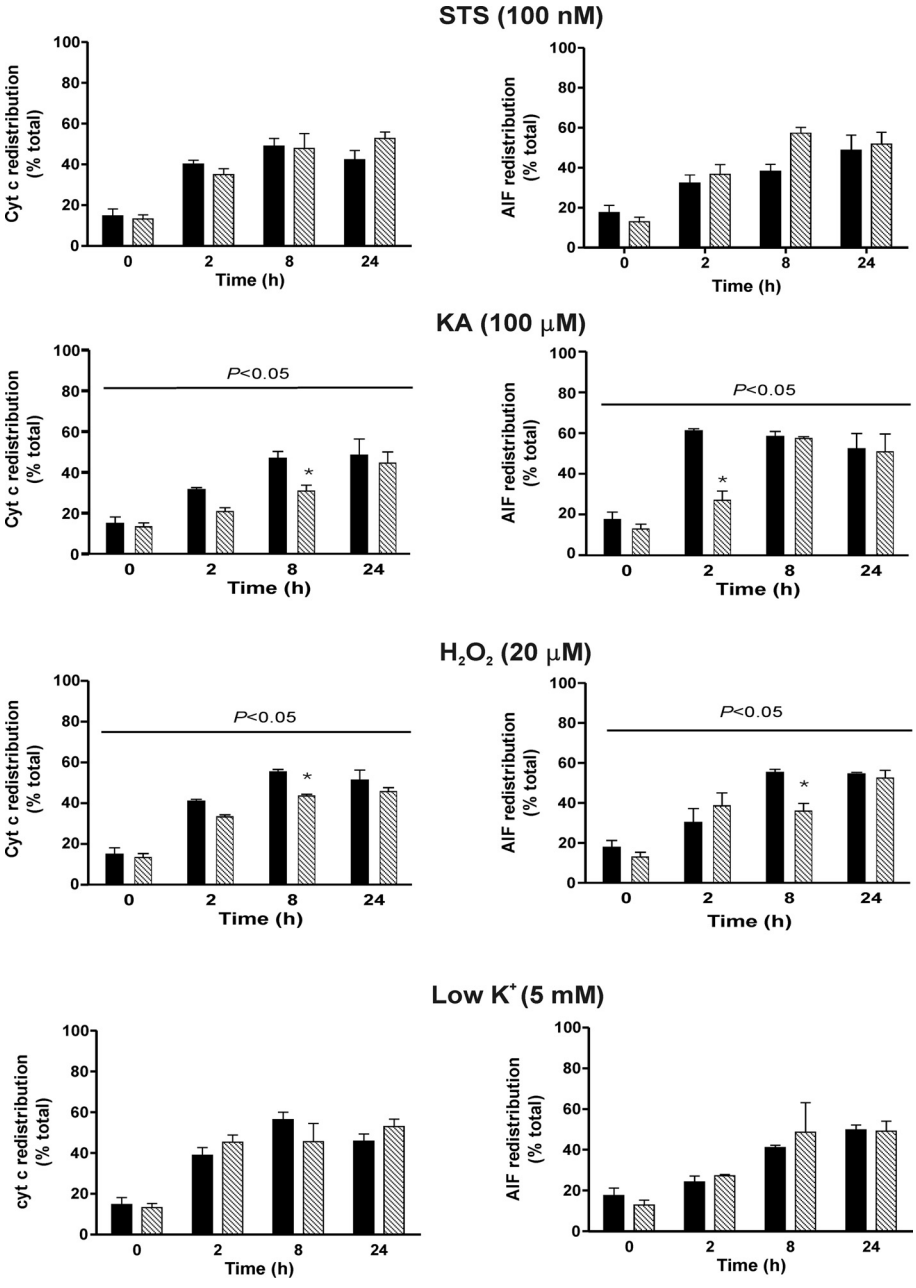

Figure 6. Inhibition of calpains affects redistribution of mitochondrial proteins. The redistribution of cyt c and AIF were individually monitored in cells treated with STS, KA, H_2O_2 and low K^+. Treatments were carried out in the absence (black bars) and presence of calpastatin peptide (5 μM; diagonal bars). Data represent the overall proportion of cells scored for redistribution of cyt c and AIF and are a mean ± SEM of four data sets, 250–500 cells/time point. Horizontal lines indicate statistically significant differences between presence and absence of calpastatin within an individual insult-treated set of timepoints. Asterisks indicate significant differences relative to the appropriate control group at individual timepoints ($P<0.05$).

the late activation of caspase-3, indicating some measure of caspase participation in cell death, the increase in number of HtrA2/Omi- and AIF- redistributing cells between 6–8 h suggests that H_2O_2-induced cell death involves an appreciable caspase-independent component. Although the concurrent activation of caspase-dependent and caspase-independent mechanisms has been observed in other forms of neuronal injury [24, 36, 37], there is a general paucity of information in this area. Of those cells which showed protein redistribution in the period 2–6 h after KA treatment, the majority of cells treated with KA redistributed HtrA2/Omi and AIF prior to cyt c and Smac/DIABLO over 2–6 h, indicative of a largely caspase-independent mode of cell death. These results are in agreement with other studies that have shown the redistribution of AIF prior to cyt c [14, 38] and the prominent role AIF plays in excitotoxic injury [39] downstream of free radical generation [6, 9]. In addition, studies suggest that AIF can act on mitochondria to induce the release of cyt c and additional AIF, leading to a feed-forward amplification cascade [40]. Therefore, it is possible that cyt c redistribution after KA exposure is a consequence of AIF redistribution. Moreover, the depletion of mitochondrial AIF may exacerbate oxidative injury due to

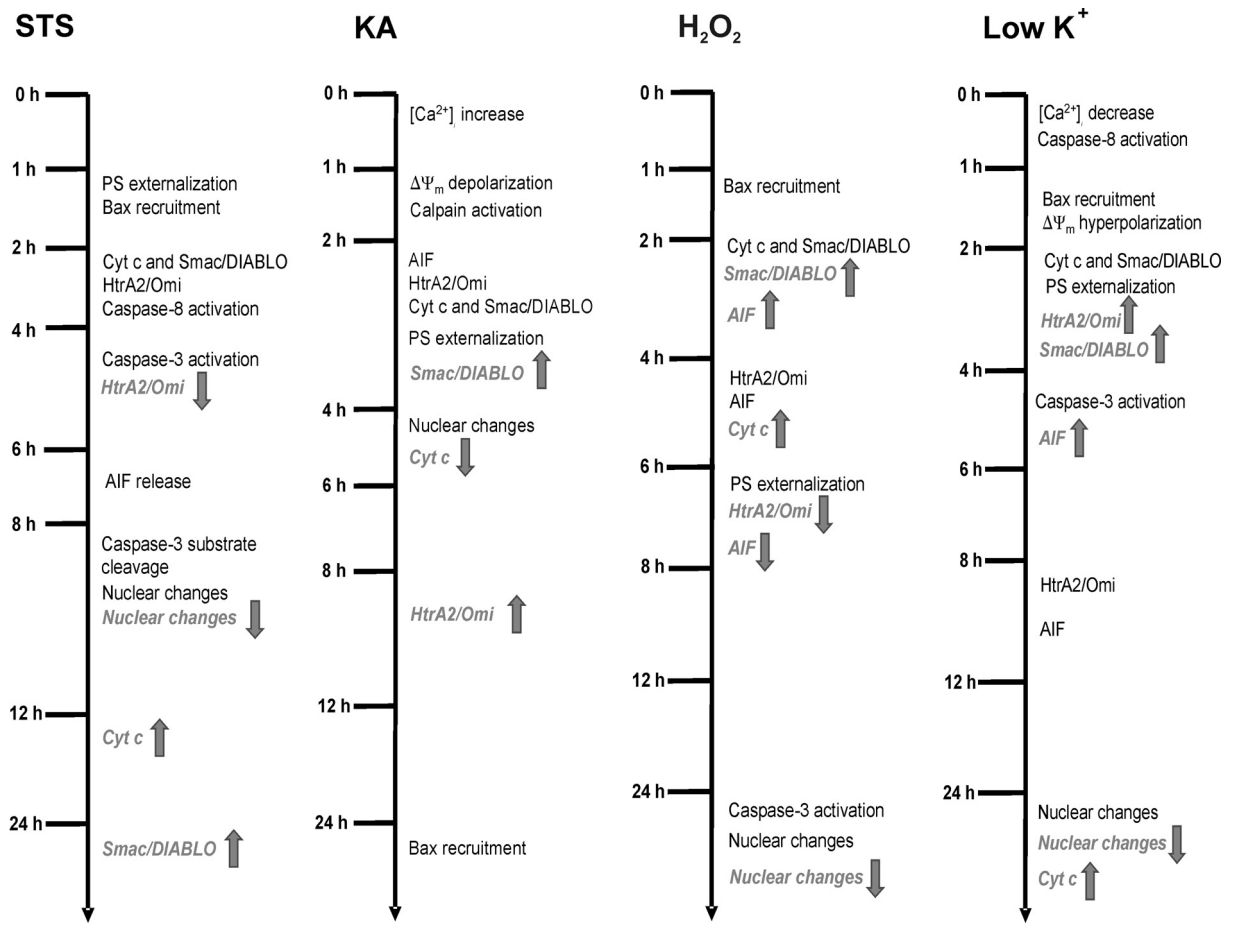

Figure 7. Timelines for the key PCD events in neurons treated with STS, KA, H_2O_2 and low K^+. Grey italics indicate the effect of caspase inhibition.

minimization of is protective role in this organelle. It is noteworthy that of all the stressors applied here KA treatment led to the most rapid decline of mitochondrial function, perhaps reflective of the earliest redistribution of AIF from mitochondria (Fig. 3B).

In the presence of zVAD-fmk, neuronal death continued, suggesting that caspase-independent pathways can compensate for caspase-dependent events when the caspase cascade is blocked. Such findings are consistent with evidence for the redundancy of cell death pathways when cells are stressed to the point of death [20, 41, 42]. As previously shown [24, 43], cyt c redistribution could not be attenuated in the presence of zVAD-fmk and was therefore observed to be caspase-independent, particularly during STS-, H_2O_2- and low K^+-induced cell death. Under our conditions Smac/DIABLO redistribution is relatively caspase-independent, in agreement with previous studies [25, 44]. In fact, zVAD-fmk increased the redistribution of Smac/DIABLO for all insults (Fig. 4C), indicating a possible feed-forward loop. The late activation of caspase-3 and the prominent role of AIF during H_2O_2-induced cell death suggests that H_2O_2 triggers the activation of both caspase-dependent and caspase-independent pathways. Initially, cell death induced by H_2O_2 was cyt c- and Smac/DIABLO-mediated, however after 4 h a more caspase-independent process was activated with the substantial redistribution of HtrA2/Omi and AIF. Our extensive data on the different profiles of IMS protein redistribution, and their modulation by protease inhibition, exemplify the contemporary understanding of OMM permeabilization wherein release of IMS proteins is context-dependent [10]. Overall these results provide new support for the differential canonical redistribution of IMS proteins which are diversely recruited in a stressor-dependent manner to mitochondrial-dependent PCD (Fig. 7).

Possible triggers of mitochondrial protein release. Bax has been shown to be recruited to the OMM following an apoptotic stimulus and to promote mitochondrial protein redistribution [6, 7]. Treatment with STS, H_2O_2 and low K^+ resulted in recruitment of Bax to the OMM

prior to IMS protein release. The subsequent timing of mitochondrial IMS protein release relative to the translocation of Bax to the OMM, suggests that Bax mediates protein redistribution under these conditions. KA exposure induced late recruitment of Bax to the OMM, in agreement with other studies [45, 46]. Thus, Bax does not play a crucial role during KA-induced excitotoxic injury, and hence injury progress may solely involve components of the mPTP, perhaps associated with AIF release [6] or other pore forming mitochondrial proteins such as Bak [47]. However, previous studies have shown that Ca^{2+} is an early mediator of neuronal injury and may trigger downstream events, such as mitochondrial depolarization [27, 48]. Interestingly, KA exposure resulted in a rapid rise of $[Ca^{2+}]_i$ followed by $\Delta\Psi_m$ depolarization. Therefore, after KA exposure, the increase in $[Ca^{2+}]_i$ may trigger mPTP opening, $\Delta\Psi_m$ loss and subsequent release of mitochondrial IMS proteins.

Calpain- and AIF-mediated cell death after excitotoxic injury. Caspase inhibition was insufficient to completely protect neurons from cell death and only attenuated cell death in response to STS, H_2O_2 and low K^+, indicating the activation of other cell death components [41]. This idea was confirmed after calpain inhibition studies, which effected considerable neuroprotection after KA and H_2O_2 injury. However, like pan-caspase inhibition by zVAD-fmk, calpain inhibition only delayed the cell death process, indicating the complexity of apoptotic pathways and cellular commitment to die [41, 42].

Calpain activation contributes to neuronal loss involving apoptotic injury in various pathological conditions [49], KA-mediated excitotoxicity [50] and stroke injury [15]. Calpains also interact with AIF and enhance its release from mitochondria by cleaving Bid into its active truncated form [17]. Indeed, calpain inhibition attenuated AIF release following KA- and H_2O_2-mediated injury. Although caspases have been shown to be involved in some forms of excitotoxicity via glutamate receptor activation [51], they do not seem to be involved herein in cell death induced by KA, since caspase inhibition is not neuroprotective and calpain activation predominates in mature neurons [50]. Our analyses of KA-treated cells suggests that the rapid rise in $[Ca^{2+}]_i$ activates calpains directly, or disrupts physiological processes that regulate calpains [49]. Activation of calpains inhibits caspase activation via their direct cleavage [52], and this action may explain why KA-induced cell death is caspase-independent.

Our detailed analyses of neuronal PCD using "neurologic stressors" allowed us to define the engagement of death machinery. Regardless of the stressor employed, we found redistribution of mitochondrial IMS proteins in an insult-dependent manner, with differential interplay between caspase-dependent and caspase-independent signaling (Fig. 7). These data provide novel insights relevant to a growing body of evidence for diverse signatures for PCD during neuronal injury [8, 37, 53]. Moreover our findings support the idea of redundant pathways of cellular demise during neuronal PCD [42, 54] and the concepts of the evolutionary development of multiple PCD pathways.

Acknowledgements. We thank the staff of Monash University Micro Imaging Facility for technical assistance and Dr. Joanne Britto for her advice on real-time imaging. This work was supported by the NH&MRC (Australia) (Program 236805, Project 509217) and by the Australian Research Council. SD was a Dora Lush Scholar and PMB a Senior Principal Research Fellow of the NH&MRC (Australia)

1 Tatton, W. G. and Olanow, C. W. (1999) Apoptosis in neurodegenerative diseases: the role of mitochondria. Biochim. Biophys. Acta. 1410, 195–213.
2 Beal, M. F. (2005) Mitochondria take center stage in aging and neurodegeneration. Ann. Neurol. 58, 495–505.
3 Green, D. and Kroemer, G. (1998) The central executioners of apoptosis: caspases or mitochondria? Trends Cell Biol. 8, 267–271.
4 Lim, M. L., Mercer, L. D., Nagley, P. and Beart, P.M. (2007) Rotenone and MPP+ preferentially redistribute apoptosis-inducing factor in apoptotic dopamine neurons. Neuroreport. 18, 307–312.
5 Polster, B. M. and Fiskum, G. (2004) Mitochondrial mechanisms of neural cell apoptosis. J. Neurochem. 90, 1281–1289.
6 Kroemer, G., Galluzzi, L. and Brenner, C. (2007) Mitochondrial membrane permeabilization in cell death. Physiol. Rev. 87, 99–163.
7 Lim, M. L., Lum, M. G., Hansen, T. M., Roucou, X. and Nagley, P. (2002) On the release of cytochrome c from mitochondria during cell death signaling. J. Biomed. Sci. 9, 488–506.
8 Ankarcrona, M., Dypbukt, J. M., Bonfoco, E., Zhivotovsky, B., Orrenius, S., Lipton, S. A. and Nicotera, P. (1995) Glutamate-induced neuronal death: a succession of necrosis or apoptosis depending on mitochondrial function. Neuron. 15, 961–973.
9 Luetjens, C. M., Bui, N. T., Sengpiel, B., Munstermann, G., Poppe, M., Krohn, A. J., Bauerbach, E., Krieglstein, J. and Prehn, J. H. (2000) Delayed mitochondrial dysfunction in excitotoxic neuron death: cytochrome c release and a secondary increase in superoxide production. J. Neurosci. 20, 5715–5723.
10 Smith, D. J., Ng, H., Kluck, R. M. and Nagley, P. (2008) The mitochondrial gateway to cell death. IUBMB Life. 60, 383–389.
11 Hardwick, J. M. and Polster, B. M. (2002) Bax, along with lipid conspirators, allows cytochrome c to escape mitochondria. Mol. Cell. 10, 963–965.
12 Gill, M. B. and Perez-Polo, J. R. (2008) Hypoxia ischemia-mediated cell death in neonatal rat brain. Neurochem. Res.
13 Zhang, Z., Yang, X., Zhang, S., Ma, X. and Kong, J. (2007) BNIP3 upregulation and EndoG translocation in delayed neuronal death in stroke and in hypoxia. Stroke. 38, 1606–1613.
14 Cande, C., Vahsen, N., Garrido, C. and Kroemer, G. (2004) Apoptosis-inducing factor (AIF): caspase-independent after all. Cell Death Differ. 11, 591–595.

15 Blomgren, K., Leist, M. and Groc, L. (2007) Pathological apoptosis in the developing brain. Apoptosis. 12, 993–1010.
16 Orrenius, S., Zhivotovsky, B. and Nicotera, P. (2003) Regulation of cell death: the calcium-apoptosis link. Nat. Rev. Mol. Cell Biol. 4, 552–565.
17 Polster, B. M., Basanez, G., Etxebarria, A., Hardwick, J. M. and Nicholls, D. G. (2005) Calpain I induces cleavage and release of apoptosis-inducing factor from isolated mitochondria. J. Biol. Chem. 280, 6447–6454.
18 Yu, S. W., Wang, H., Poitras, M. F., Coombs, C., Bowers, W. J., Federoff, H. J., Poirier, G. G., Dawson, T. M. and Dawson, V. L. (2002) Mediation of poly(ADP-ribose) polymerase-1-dependent cell death by apoptosis-inducing factor. Science. 297, 259–263.
19 Yu, S. W., Wang, H., Dawson, T. M. and Dawson, V. L. (2003) Poly(ADP-ribose) polymerase-1 and apoptosis inducing factor in neurotoxicity. Neurobiol. Dis. 14, 303–317.
20 Degterev, A. and Yuan, J. (2008) Expansion and evolution of cell death programmes. Nat. Rev. Mol. Cell Biol. 9, 378–390.
21 Clarke, P. G. (1990) Developmental cell death: morphological diversity and multiple mechanisms. Anat. Embryol. (Berl). 181, 195–213.
22 Giardina, S. F., Cheung, N. S., Reid, M. T. and Beart, P. M. (1998) Kainate-induced apoptosis in cultured murine cerebellar granule cells elevates expression of the cell cycle gene cyclin D1. J. Neurochem. 71, 1325–1328.
23 D'Mello, S. R., Galli, C., Ciotti, T. and Calissano, P. (1993) Induction of apoptosis in cerebellar granule neurons by low potassium: inhibition of death by insulin-like growth factor I and cAMP. Proc. Natl. Acad. Sci. USA. 90, 10989–10993.
24 Beart, P. M., Lim, M. L., Chen, B., Diwakarla, S., Mercer, L. D., Cheung, N. S. and Nagley, P. (2007) Hierarchical recruitment by AMPA but not staurosporine of pro-apoptotic mitochondrial signaling in cultured cortical neurons: evidence for caspase-dependent/independent cross-talk. J. Neurochem. 103, 2408–2427.
25 Lim, M. L., Chen, B., Beart, P. M. and Nagley, P. (2006) Relative timing of redistribution of cytochrome c and Smac/DIABLO from mitochondria during apoptosis assessed by double immunocytochemistry on mammalian cells. Exp. Cell Res. 312, 1174–1184.
26 Cheung, N. S., Pascoe, C. J., Giardina, S. F., John, C. A. and Beart, P. M. (1998) Micromolar L-glutamate induces extensive apoptosis in an apoptotic-necrotic continuum of insult-dependent, excitotoxic injury in cultured cortical neurones. Neuropharmacology. 37, 1419–1429.
27 Rego, A. C., Ward, M. W. and Nicholls, D. G. (2001) Mitochondria control ampa/kainate receptor-induced cytoplasmic calcium deregulation in rat cerebellar granule cells. J. Neurosci. 21, 1893–1901.
28 Giardina, S. F. and Beart, P. M. (2001) Excitotoxic profiles of novel, low-affinity kainate receptor agonists in primary cultures of murine cerebellar granule cells. Neuropharmacology. 41, 421–432.
29 Assefa, Z., Bultynck, G., Szlufcik, K., Nadif Kasri, N., Vermassen, E., Goris, J., Missiaen, L., Callewaert, G., Parys, J. B. and De Smedt, H. (2004) Caspase-3-induced truncation of type 1 inositol trisphosphate receptor accelerates apoptotic cell death and induces inositol trisphosphate-independent calcium release during apoptosis. J. Biol. Chem. 279, 43227–43236.
30 Wu, H. Y., Tomizawa, K., Oda, Y., Wei, F. Y., Lu, Y. F., Matsushita, M., Li, S. T., Moriwaki, A. and Matsui, H. (2004) Critical role of calpain-mediated cleavage of calcineurin in excitotoxic neurodegeneration. J. Biol. Chem. 279, 4929–4940.
31 Nath, R., Raser, K. J., Stafford, D., Hajimohammadreza, I., Posner, A., Allen, H., Talanian, R. V., Yuen, P., Gilbertsen, R. B. and Wang, K. K. (1996) Non-erythroid alpha-spectrin breakdown by calpain and interleukin 1 beta-converting-enzyme-like protease(s) in apoptotic cells: contributory roles of both protease families in neuronal apoptosis. Biochem. J. 319 (Pt 3), 683–690.
32 Atlante, A., Calissano, P., Bobba, A., Giannattasio, S., Marra, E. and Passarella, S. (2001) Glutamate neurotoxicity, oxidative stress and mitochondria. FEBS Lett. 497, 1–5.
33 Arnoult, D., Parone, P., Martinou, J. C., Antonsson, B., Estaquier, J. and Ameisen, J. C. (2002) Mitochondrial release of apoptosis-inducing factor occurs downstream of cytochrome c release in response to several proapoptotic stimuli. J. Cell Biol. 159, 923–929.
34 Du, C., Fang, M., Li, Y., Li, L. and Wang, X. (2000) Smac, a mitochondrial protein that promotes cytochrome c-dependent caspase activation by eliminating IAP inhibition. Cell. 102, 33–42.
35 Verhagen, A. M., Ekert, P. G., Pakusch, M., Silke, J., Connolly, L. M., Reid, G. E., Moritz, R. L., Simpson, R. J. and Vaux, D. L. (2000) Identification of DIABLO, a mammalian protein that promotes apoptosis by binding to and antagonizing IAP proteins. Cell. 102, 43–53.
36 Cadet, J. L., Jayanthi, S. and Deng, X. (2003) Speed kills: cellular and molecular bases of methamphetamine-induced nerve terminal degeneration and neuronal apoptosis. Faseb J. 17, 1775–1788.
37 Volbracht, C., Chua, B. T., Ng, C. P., Bahr, B. A., Hong, W. and Li, P. (2005) The critical role of calpain versus caspase activation in excitotoxic injury induced by nitric oxide. J. Neurochem. 93, 1280–1292.
38 Daugas, E., Susin, S. A., Zamzami, N., Ferri, K. F., Irinopoulou, T., Larochette, N., Prevost, M. C., Leber, B., Andrews, D., Penninger, J. and Kroemer, G. (2000) Mitochondrio-nuclear translocation of AIF in apoptosis and necrosis. Faseb J. 14, 729–739.
39 Wang, H., Yu, S. W., Koh, D. W., Lew, J., Coombs, C., Bowers, W., Federoff, H. J., Poirier, G. G., Dawson, T. M. and Dawson, V. L. (2004) Apoptosis-inducing factor substitutes for caspase executioners in NMDA-triggered excitotoxic neuronal death. J. Neurosci. 24, 10963–10973.
40 Susin, S. A., Lorenzo, H. K., Zamzami, N., Marzo, I., Snow, B. E., Brothers, G. M., Mangion, J., Jacotot, E., Costantini, P., Loeffler, M., Larochette, N., Goodlett, D. R., Aebersold, R., Siderovski, D. P., Penninger, J. M. and Kroemer, G. (1999) Molecular characterization of mitochondrial apoptosis-inducing factor. Nature. 397, 441–446.
41 Yuan, J., Lipinski, M. and Degterev, A. (2003) Diversity in the mechanisms of neuronal cell death. Neuron. 40, 401–413.
42 Leist, M. and Jaattela, M. (2001) Triggering of apoptosis by cathepsins. Cell Death Differ. 8, 324–326.
43 Deshmukh, M., Kuida, K. and Johnson, E. M., Jr. (2000) Caspase inhibition extends the commitment to neuronal death beyond cytochrome c release to the point of mitochondrial depolarization. J. Cell Biol. 150, 131–143.
44 Zhou, L. L., Zhou, L. Y., Luo, K. Q. and Chang, D. C. (2005) Smac/DIABLO and cytochrome c are released from mitochondria through a similar mechanism during UV-induced apoptosis. Apoptosis. 10, 289–299.
45 Miller, T. M., Moulder, K. L., Knudson, C. M., Creedon, D. J., Deshmukh, M., Korsmeyer, S. J. and Johnson, E. M., Jr. (1997) Bax deletion further orders the cell death pathway in cerebellar granule cells and suggests a caspase-independent pathway to cell death. J. Cell Biol. 139, 205–217.
46 Cheung, E. C., Melanson-Drapeau, L., Cregan, S. P., Vanderluit, J. L., Ferguson, K. L., McIntosh, W. C., Park, D. S., Bennett, S. A. and Slack, R. S. (2005) Apoptosis-inducing factor is a key factor in neuronal cell death propagated by BAX-dependent and BAX-independent mechanisms. J. Neurosci. 25, 1324–1334.
47 Brustovetsky, N., Dubinsky, J. M., Antonsson, B. and Jemmerson, R. (2003) Two pathways for tBID-induced cytochrome c release from rat brain mitochondria: BAK- versus BAX-dependence. J. Neurochem. 84, 196–207.
48 Budd, S. L. and Nicholls, D. G. (1996) Mitochondria, calcium regulation, and acute glutamate excitotoxicity in cultured cerebellar granule cells. J. Neurochem. 67, 2282–2291.

49 Goll, D. E., Thompson, V. F., Li, H., Wei, W. and Cong, J. (2003) The calpain system. Physiol. Rev. 83, 731–801.
50 Takano, J., Tomioka, M., Tsubuki, S., Higuchi, M., Iwata, N., Itohara, S., Maki, M. and Saido, T. C. (2005) Calpain mediates excitotoxic DNA fragmentation via mitochondrial pathways in adult brains: evidence from calpastatin mutant mice. J. Biol. Chem. 280, 16175–16184.
51 Du, Y., Bales, K. R., Dodel, R. C., Hamilton-Byrd, E., Horn, J. W., Czilli, D. L., Simmons, L. K., Ni, B. and Paul, S. M. (1997) Activation of a caspase 3-related cysteine protease is required for glutamate-mediated apoptosis of cultured cerebellar granule neurons. Proc. Natl. Acad. Sci. USA. 94, 11657–11662.
52 Bizat, N., Hermel, J. M., Humbert, S., Jacquard, C., Creminon, C., Escartin, C., Saudou, F., Krajewski, S., Hantraye, P. and Brouillet, E. (2003) In vivo calpain/caspase cross-talk during 3-nitropropionic acid-induced striatal degeneration: implication of a calpain-mediated cleavage of active caspase-3. J. Biol. Chem. 278, 43245–43253.
53 Cheung, N. S., Peng, Z. F., Chen, M. J., Moore, P. K. and Whiteman, M. (2007) Hydrogen sulfide induced neuronal death occurs via glutamate receptor and is associated with calpain activation and lysosomal rupture in mouse primary cortical neurons. Neuropharmacology. 53, 505–514.
54 Susin, S. A., Daugas, E., Ravagnan, L., Samejima, K., Zamzami, N., Loeffler, M., Costantini, P., Ferri, K. F., Irinopoulou, T., Prevost, M. C., Brothers, G., Mak, T. W., Penninger, J., Earnshaw, W. C. and Kroemer, G. (2000) Two distinct pathways leading to nuclear apoptosis. J. Exp. Med. 192, 571–580.